

Comparison of fatigue performances of gapped and partially overlapped CHS K-joints

Sopha, T.; Lee, Chi King; Chiew, Sing Ping; Lie, Seng Tjhen

2011

Lee, C. K., Chiew, S. P., Lie, S. T., & Sopha, T. (2011). Comparison of fatigue performances of gapped and partially overlapped CHS K-joints. *Engineering Structures*, 33(1), 44-52.

<https://hdl.handle.net/10356/102228>

<https://doi.org/10.1016/j.engstruct.2010.09.016>

© 2011 Elsevier. This is the author created version of a work that has been peer reviewed and accepted for publication by *Engineering Structures*, Elsevier. It incorporates referee's comments but changes resulting from the publishing process, such as copyediting, structural formatting, may not be reflected in this document. The published version is available at: [DOI: <http://dx.doi.org/10.1016/j.engstruct.2010.09.016>].

Downloaded on 20 Mar 2024 19:09:45 SGT

COMPARISON OF FATIGUE PERFORMANCES OF GAPPED AND PARTIALLY OVERLAPPED CHS K-JOINTS

¹*C. K. Lee, S. P. Chiew, S. T. Lie and T. Sopha*

School of Civil and Environmental Engineering

Nanyang Technological University

50 Nanyang Avenue, Singapore 639798

Abstract

In this paper, a parametric numerical study is conducted to compare the fatigue performances of gapped and partially overlapped circular hollow section (CHS) K-joints under different loading conditions. In order to obtain a more complete understanding of the fatigue performances of these two joint types, the maximum stress concentrated factor (SCF), the hot spot stress (HSS) and the predicted fatigue life for a set of selected gapped and partially overlapped CHS K-joints which cover a wide range of geometrical parameters are determined and compared. For the gapped CHS K-joints, their SCF, HSS and fatigue life are obtained by using parametric equations from standard design guideline. For partially overlapped joints, since no reliable parametric equation is available, their SCF, HSS and fatigue life are obtained from a validated finite element modelling procedure. The comparison results showed that the partially overlapped CHS K-joints are able to outperform their gapped counterparts under pure or dominating axially loadings while the reverse is true when the joints are subjected to pure or dominating in-plane bending loadings.

Keywords: Fatigue life, Stress concentration factor, Hot spot stress, Gapped CHS K-joints , Partially overlapped CHS K-joints

¹ Corresponding Author.

Email: ccklee@ntu.edu.sg

Tel: 65-67905293

Fax: 65-67921650

1. Introduction

Due to the ease of fabrication and the availability of many assessment methods for ultimate strength and fatigue performance, gapped K-joints are widely used for the construction of many tubular structures. However, when the brace to chord diameters ratio, β , is higher than 0.7, gapped K-joints may not be easily designed due to the limited range of validity of many design codes [1-3] and a partially overlapped joint (joints with overlapping ratio between 25% to 75%) may be needed instead. In general, a partially overlapped CHS K-joint has a higher fabrication cost than a gapped joint due to the more complex intersection profile and construction procedure. However, in terms of ultimate strength capacity, a partially overlapped CHS K-joint is generally higher than its gapped counterpart due to the more compact connection and optimized load transfer pattern [4]. In fact, in a study comparing the costs of three K-joints design options [5], it was found that for the same ultimate strength requirement, the partially overlapped joint is the cheapest option, with the fabrication cost lower than that of the gapped joint which needs a larger and thicker CHS sections. While it is clear that partially overlapped joints could outperform their gapped counterparts in terms of ultimate static strength, only a few small scale studies were carried out to compare the fatigue performances between these two type of joints. Bouwkamp [4] reported that the stress concentration factors (SCF) of overlapped CHS K-joints could be 30% lower than those of gapped CHS K-joints having the same parameters and properties. In addition, Fessler et al. [6] reported that the hot spot stress (HSS) could be reduced as much as 40%-45% by switching from a gapped joint design to an overlapped joint design. In terms of fatigue strength, Gibstein [7] reported that improvements could be obtained by using a partially overlapped joint with same chord and brace diameters. For the development SCF and HSS equations for partially overlapped joint, Efthymiou and Durkin [8] published their equations based on a small scale finite element study involving 100 joint configurations and loading cases. Their equations were verified experimentally by Dharmavasan and Seneviratne [9] using scaled down acrylic models and it was found that overlapping may help to reduce the chord SCF. However, a recent study by Sopha et al. [10] during full scale testing found that

Ethymiou's formulae [8] are conservative only when the joints were subjected to in-plane bending loading, but not for the case of axial loading. In addition, it was also found that the HSS may be located on the brace side of the joint and this agreed with the observations by Moe [11]. This implies that the fatigue failure mode of a partially overlapped CHS K-joint could be different from a gapped joint in which the chord fatigue failure almost always determines the fatigue life. Research on fatigue behaviour of overlapped tubular K joints with an overlapping ratio larger than 50% can be found in the works done by Gho et al. [12, 13] Gao et al. [14] and Pang et al. [15]. In addition, Mashiri et al. [16] studied the SCF and fatigue behavior of thin-walled CHS and square hollow section T-joints under in-plane bending loading.

The main objective of this paper is to carry out a systematic study to assess and compare the general fatigue performances of gapped and partial overlapped CHS K-joints. The fatigue performances of these two joint types shall be compared by a parametric study in which some key fatigue performance criteria including the SCF, the HSS and the fatigue life (number of constant amplitude cyclic loadings to fatigue failure) are evaluated. It should be stressed that the objective of this paper is *not* to advocate the use of partially overlapped CHS K-joint (or vice versa) but rather to find out the relative merits of these two joint types under different loading combinations.

In the next section, the basic notations and the scope of study are introduced. They are then followed by a concise summary of the fatigue performance comparison method adopted. After that, the comparison results and findings are presented while in the last section conclusions from the present study are given.

2 Basic notations and scope of study

2.1 Basic notations and joint configurations

Fig. 1 shows the general joint configurations for the gapped and partially overlapped CHS K-joints and the parameters used for the descriptions of the joints' geometries. Essentially the same set of notations is used for both joint types except that ζ and O_v are employed

to denote the gap ratio and the overlapping ratio for the gapped and partially overlapped joints, respectively.

2.2 Range of geometrical parameters selected

Since gapped and overlapped joints are two alternative and, to some extent, competing joint configurations, in order to make the comparison study with relevant reference values, care is needed when selecting the geometrical parameters of the joints. In this study, the CHS sections used for the construction of all gapped and partially overlapped CHS K-joints were specially selected in such a way that if the gapped joints were created, they will produce high eccentricities just within the allowable limits specified in the design guideline [2]. However, if the joints are created as overlapped joints from the same sections, the eccentricity could be reduced to zero. Note that such a selection of geometrical parameters is *not* to favour the performance of the overlapped joints but on the contrary, it implies that structural engineers *prefer* to use gapped joints whenever it is possible and only consider the option of partially overlapping joints for those limited cases when the gapped joints would result in a high eccentricity.

In this study, 642 pairs of CHS K-joint configurations are considered and their geometrical parameters are listed in Table 1. Furthermore, only partially overlapped CHS K-joints with identical overlap and through braces and same intersection angles are considered as they are the most commonly encountered configurations. Hence, for all the joints, $\theta = \theta_1 = \theta_2$, $\beta = \beta_1 = \beta_2$ and $\tau = \tau_1 = \tau_2$. The geometrical parameters of the gapped CHS K-joints are also taken from the same table, but they are made with minimum gap distance. As shown in Table 1, in order to present their geometrical ranges systematically, these 642 pairs of K-joints are divided into 14 groups purely based on their β values. For each group, a suitable chord diameter (D) is selected and a series of γ (or chord thickness) values are adopted. For each γ value, different sets of τ values (last column of Table 1) are employed so that the brace shall correspond to realistic CHS dimensions. As shown in the last column of Table 1, larger chord thickness (higher γ values) shall normally lead to a larger set of τ values for the obvious reason that more choices of brace thickness are available. Finally,

suitable pairs of overlapping ratio (O_v) and intersection angle (θ) are selected. It should be mentioned that according to the study by Nguyen [17], high eccentricity gapped K-joints are frequently occurred when $\theta \geq 45^\circ$ with $\beta \geq 0.65$ as shown in the second and third columns of Table 1.

3 Methodology for the fatigue performance comparison

In this study, the following three key fatigue performance criteria of the joints are evaluated and compared.

3.1 Comparison of the maximum SCF under different basic loading cases

Since a joint with a higher maximum SCF generally implies a higher HSS, the maximum SCF attained under a certain basic load case could be a useful indicator for the fatigue performance of the joint. In this study, for the partially overlapped joint, four basic load cases, namely AX1, IPB1, AX2 and IPB2 were studied. As shown in Fig. 1b, AX1 and AX2 are the basic axial (AX) loads applied at the ends of the through and the overlap braces, respectively. Similarly, IPB1 and IPB2 are, respectively, the corresponding in-plane bending (IPB) loads applied at the ends of the through and the overlap braces. It should be noted that the directions of the IPB1 and IPB2 load cases are selected such that maximum SCF shall be induced at the weld toe along the brace-chord intersection curve [10]. For the corresponding gapped joints, due to symmetry, only the AX1 and IPB1 load cases were applied at the end of one of the brace. In all cases, the ends of the chord are assumed to be fully fixed and no loading was applied to the chord. Note that in reality, different levels of chord loadings are often found in many tubular structures (e.g. trusses). However, in order to limit the number of comparisons within a manageable level, no chord loading was applied and the only the effects of different brace loadings were considered in this study.

3.1.1 Calculation of SCF for gapped CHS K-joints

In order to carry out the comparison study, it is necessary to obtain the SCF expressions of the joints. For the calculation of SCF for gapped CHS K-joints, different forms of SCF equations were suggested in the past few decades by Kuang et al. [18], Wordsworth and Smedley [19, 20], Efthymiou and Durkin [8], Smedley and Fisher [21], Karamanos et al. [22] and Zhao et al. [2]. In this study, the SCF equations suggested by Smedley and Fisher [21] were employed. These equations, which are commonly referred as the DEn SCF equations as they were developed in a research project sponsored by the UK Department of Energy, were selected as it was found that they are more accurate than those equations suggested by Kuang et al. [18], Wordsworth and Smedley [19, 20] as well as Efthymiou and Durkin [8]. Furthermore, those equations suggested by Karamanos et al. [22] and Zhao et al. [2] are, in fact, simplified and shortened forms of the DEn equations. In addition, works results obtained from Schumacher [23, 24] concluded that those equations suggested by Karamanos et al. [22] were on the conservative side for joints with γ values equal to 12. The DEn SCF equations for gapped CHS K-joints with identical braces are listed in Tables 2a and 2b. The maximum SCF for each joint is obtained by checking the SCF obtained from different brace and chord positions shown in Table 2. It should be noted that for Table 2, the valid range of the γ value is $10 \leq \gamma \leq 35$. However, from Table 1 one can see that γ value as low as 5.82 could be found. In order to deal with this out-of-range problem, in this study, the lower limit of the application range of Table 2 was slightly extended to $\gamma=8.0$. While for joints with γ value less than 8.0, 3D solid finite element models were created by using the automatic mesh generation scheme developed by Lie et al. [25] so that the maximum SCF value for the gapped joints with low γ value could be extracted by the standard extrapolation method [2].

3.1.2 Calculation of SCF for partially overlapped CHS K-joints

For the calculation of SCF for partially overlapped CHS K-joints, due to the complexity of this joint type, only the equations reported by Efthymiou and Durkin [8] are available from the literature. However, as they were found to be not conservative for the AX loading case

[10, 17, 26], they were not adopted in this study. In order to obtain reliable SCF for partially overlapped CHS K-joint, a special automatic mesh generation procedure developed by Nguyen et al. [17, 27, 28] was employed to create well graded 3D solid finite element meshes including welding details (Fig. 2a) for the 642 joints studied. The maximum SCF of the joints were then extracted from the finite element stress analyses results (Fig. 2b) using an appropriate extrapolation technique [2, 17, 26-28]. While such direct analysis procedure appears to be expensive and time consuming, it turns out that after the automatic mesh generation and stress extraction procedures are developed [17, 26-28], accurate estimations of SCF and HSS for a partially overlapped or a gapped CHS K-joint could be determined within 20 mins on a low-end PC.

3.2 Comparison of the HSS under combined AX and IPB loadings

Since in general the fatigue life of a tubular joint will be reduced as its HSS increases, another possible method to assess the fatigue performance is to compare the HSS of the pairs of sample joints. As the HSS induced will be affected by the loading applied, the following five loading cases were considered:

- (i) Pure AX1 loading of 200kN.
- (ii) Pure IPB1 loading of 45kNm.
- (iii) Combined loading of AX1 (200kN) and IPB1 (10kNm).
- (iv) Combined loading of AX1 (200kN) and IPB1 (25kNm).
- (v) Combined loading of AX1 (200kN) and IPB1 (45kNm).

Obviously, the pure AX1 and IPB1 loadings were employed to study the relative fatigue performance of the two joint types under the basic loading cases while the combined loadings were employed to study the effects of IPB loading. Note that the values of IPB in the combined loading cases were capped to a relatively small value of 45kNm. This is because the design code would implicitly limit the magnitude of IPB loading by specifying the maximum eccentricity for the case of gapped joint. While for the case of partially overlapped joint, most eccentricity could have already been eliminated by the use of appropriate overlapping ratio.

In the parametric study, the actual HSS achieved in the 642 sample joints were obtained by using the SCF equations for the gapped joints with $\gamma \geq 8$ and directly extracted from the finite element analyses results for all partially overlapped joints and gapped joints with $\gamma \leq 8$.

3.3 *Comparison of the estimated fatigue life under combined AX and IPB cyclic loadings*

Since for a given HSS, the expected fatigue life is affected by the thickness of the section under concerned, the most direct method to compare the fatigue performance of the 642 sample joints is to calculate the expected fatigue life according to the CIDECT design guideline [2]. Under a constant amplitude cyclic loading, the expected fatigue life of a gapped or partially overlapped joint could be determined by the following steps:

- (i) For each of the intersection curve between the braces and the chord, determine the maximum and minimum HSS under the cyclic loading.
- (ii) Compute the corresponding HSS ranges under the cyclic loading for all the intersection curves.
- (iii) By using the standard S-N curve for CHS joints [2], estimate the expected numbers of cycles to failure for all of the intersection curves.
- (iv) The minimum numbers of cycles obtained in step (iii) is taken as the fatigue life of the joint.

In this study, five different constant amplitude cyclic loadings are considered, see section 3.2, and the cycles considered are ranging from zero load to the values given previously for the five different loading cases. Note that due to the differences of the brace and chord thicknesses of the 642 sample joints, it is expected that the results obtained from the fatigue life comparison are not identical with those obtained in the HSS comparison.

4. Comparison results

4.1 Comparison of SCF

In order to compare the relative performance in terms of the maximum SCF induced by basic loading cases, the relative differences between the maximum SCF, $D_{Ov-Gap}(SCF)$, defined as

$$D_{Ov-Gap}(SCF) = \frac{SCF_{Ov} - SCF_{Gap}}{SCF_{Ov}} \times 100\% \quad (1)$$

are computed from the maximum SCF obtained at the chord and the loading braces. In Eqn. 1, SCF_{Ov} and SCF_{Gap} are the maximum SCF for the partially overlapped and the gapped joints, respectively. Note that from Eqn. 1, the benefit of using one of these two types of joints can be recognized by the sign of $D_{Ov-Gap}(SCF)$. A *negative* value of $D_{Ov-Gap}(SCF)$ indicates that the partially overlapped joint is better (lower SCF), while a *positive* value of $D_{Ov-Gap}(SCF)$ indicates that the gapped joint is better.

Figs. 3 to 6 illustrate the relative performances of the two joint types in terms of $D_{Ov-Gap}(SCF)$ when they are subjected to the AX and the IPB load cases. From Figs. 3 to 6, it can be seen that in the AX1 and AX2 load cases the SCF on the loading brace, for the partially overlapped CHS K-joints, are higher than that for the gapped joints, while the corresponding SCF values on the chord are lower than that for the gapped joints. In the IPB1 and IPB2 load cases, the SCF on both chord and braces, for the partially overlapped joints are usually higher than that for the gapped joints. From Figs. 3 and 5, it can be seen that the values of $D_{Ov-Gap}(SCF)$ for the AX1 and AX2 load cases on the loading braces are ranging from 4.30 % to 75.07%, while on the chord side is from -742.9% to 34.6 %. From Figs. 4 and 6, it can be seen that the values of $D_{Ov-Gap}(SCF)$ for the IPB1 and IPB2 load cases are ranging from 30.49% to 69.64% on the loading braces, while on the chord side the ranges are from -86.74% to 37.65%.

Hence, from the results obtained from maximum SCF, it seems that the partially overlapped CHS K-joints are better when working under the AX load cases, and the gapped CHS K-joints are better when working under the IPB load cases.

4.2 Comparison of HSS

Similar to the SCF comparison, the relative differences between the HSS obtained, $D_{Ov-Gap}(HSS)$, defined as

$$D_{Ov-Gap}(HSS) = \frac{HSS_{Ov} - HSS_{Gap}}{HSS_{Ov}} \times 100\% \quad (2)$$

are computed under the five loading combinations listed in Section 3.2. In Eqn. 2, HSS_{Ov} and HSS_{Gap} are the HSS for the partially overlapped and gapped joints, respectively. Again, from Eqn. 2, a *negative* $D_{Ov-Gap}(HSS)$ value indicates that the partially overlapped joint is better and *vice versa*. The $D_{Ov-Gap}(HSS)$ distributions obtained from different loading combinations are plotted in Figs. 7 to 11.

In general, locations of HSS depend on both the loading applied and the geometrical parameters of the joints and their relationships are not simple. For detailed results of the locations of the HSS locations, one may refer to reference [2] for the gapped joints and references [10] and [17] for the partially overlapped joints. However, by analyzing the HSS obtained from the two joint types, it was found that when the joints were subjected to the basic load of AX1=200kN, all HSS occurred on the chord side for the gapped joint. However, in 79.40% of the partially overlapped joints, HSS occurred on the through brace or the overlap brace side. Furthermore from Fig. 7, it is observed that the partially overlapped joints are more favorable than the gapped joints under the AX1 load case. Detailed investigations showed that 88.65% of gapped joints have higher HSS than their corresponding partially overlapped joints. Only 11.35% of partially overlapped joints, mainly those having braces with γ value higher than 12, have higher HSS than their gapped counterparts. In other words, partially overlapped joints behave better under AX load when the γ value is under 12.

For the case of IPB11=45kNm, it was found that for the gapped joints, the HSS occurred on the chord and brace sides with a proportion of 84.12% and 15.88%, respectively. While for the partially overlapped joint, the HSS occurred on the chord and the brace sides with a proportion of 23.36% and 76.64%, respectively. From Figure 8, it is observed that under pure IPB loading, the gapped joints showed better performance than the corresponding

partially overlapped joints. This observation could be attributed to the fact that partially overlapped joints are generally stiffer than the gap joints. As a result, HSS frequently occurred on the braces of the partially overlapped joints which are usually thinner than the chords, eventually higher HSS was induced there.

For the remaining three combined loading cases, it is obvious that the relative magnitudes of the AX and IPB loadings affected the results obtained. Nevertheless, it is believed that these load combinations would give some hints on the relative performances of the two joint types. In addition, it was found that even with the present of IPB loading, in all the three combined loading cases, the HSS for the gapped and partially overlapped joints still mainly occur on the chords and the braces, respectively. Plots of the distributions of $D_{Ov-Gap}(HSS)$ for the three combined loading cases are shown in Figs. 9 to 11. From these figures, it can be observed that with the increase of IPB, the benefit turned out in favor of the gapped joints. In particular, detailed analysis of the data shows that the percentage of cases where the gapped joints have higher HSS was decreased from 59.32% to 35.83% and eventually to only 18.11% when the IPB loading was increased from 10kNm to 25kNm and then to 45kNm, respectively.

From the above HSS comparison, it was observed that the relative difference of HSS between the gapped and the partially overlapped joints follows a similar pattern as in the case of SCF comparison. In particular, partially overlapped and gapped joints perform better under the AX loading and the IPB loading, respectively. However, it should be remarked that since under different loading conditions, the HSS values could occur at different intersection curves of the joint which corresponding to different sectional thicknesses. Therefore, the predicted fatigue life should also be considered so that a more complete understanding about the fatigue performance of these two types of joints could be obtained.

4.3 Comparison of predicted fatigue life

During the comparison of predicted fatigue life, $D_{Ov-Gap}(FL)$, the relative differences between the numbers of cycles to failure are computed as:

$$D_{Ov-Gap}(FL) = \frac{F_{Ov} - F_{Gap}}{F_{Ov}} \times 100\% \quad (3)$$

In Eqn. 3, F_{Ov} and F_{Gap} are, respectively, the numbers of cycles to failure estimated by using the standard S-N curve [2] for the partially overlapped and gapped CHS K-joints. From Eqn. 3, it can be seen that a *positive* value of $D_{Ov-Gap}(FL)$ indicates that the partially overlapped joint is in favor and vice versa. The distributions of $D_{Ov-Gap}(FL)$ for the five different loading combinations listed in Section 3.2 are shown in Figs. 12 to 16.

From Fig. 12, it can be seen that under the action of pure AX loading, the partially overlapped joints performed better than their gapped counterparts with 92.91% of the gapped joints failed earlier. In addition, detailed analysis of the results shown that for the 7.09% cases where the partially overlapped joints failed earlier, they all have γ values of more than 12. For the case of pure IPB loading shown in Fig. 13, it can be seen that the gapped joints is the preferred joint type as almost *all* partially overlapped joints involved in this comparison failed earlier than the corresponding gapped joints.

For the remaining combined loading cases shown in Figs. 14 to 16, a similar changing in patterns of distributions as in the case of HSS comparison could be seen: As the magnitude of the IPB component was increased from 10kNm (Fig. 14) to 25kNm (Fig. 15) and then eventually to 45kNm (Fig. 16), the percentages of cases when the gapped joint failed earlier than the partially overlapped joint were decreased from 79.92% to 43.04% and then to 21%, respectively. Hence, it could be concluded that the gapped joints will gradually become the favored joint type as the magnitude of the IPB component increases. Finally, after some detailed analyses of the data plotted in Figs. 7 to 11 with the corresponding figures in Figs. 12 to 16, it was found that the percentages of cases where the overlapped joints are in favour during HSS comparison are slightly different from that obtained during fatigue life comparison. This observation confirmed the effects of the thicknesses of the sections on the actual fatigue life of the joints. This effect can be classified as marginal.

One final remark regarding the comparison results is that as the main objective of this study is to compare the *overall* fatigue performance between the gapped and overlapped CHS K-joint under different loading cases rather than to investigate in details the effects of different geometrical parameters, no attempted was made to check for the possibility of regrouping the 14 groups of joints indicated in Table 1 to identify any correlation between the major geometrical parameters and the relative fatigue performances of the two joint types.

4.4 Implications on the design of trusses

From the practical point of view in the actual design of trusses, it is common to assume that the members are pin-ended, although some bending moments will be introduced, mostly due to misalignments between the centerlines of intersecting members at connections. Furthermore, some design manuals such as the IIW [29] recommended that these moments can be neglected during the joint design provides that the eccentricity associated with them falls within the limits stipulated in the CIDECT guide [2]. In addition, secondary bending moments are also introduced into the members due to the end fixities of the members and inherent stiffness of the joints. However, Packer et al. [30] suggested that these moments can also be ignored with respect to design of both members and joints, on the basis that there is adequate deformation and rotation capacity in both the joints and members which allow stresses to be redistributed at the ultimate limit state, or after local yielding of the joints. Therefore, based on the results presented in this study, partially overlapped K-joints could be regarded as a favorite choice when compared to gapped CHS K-joints on fatigue performance so long as the magnitude of the IPB components could be controlled by limiting the connection eccentricities within the stipulated limits by the CIDECT guide [2].

5 Conclusions

In this paper, the results obtained from the parametric numerical study on the relative fatigue performances of partially overlapped CHS K-joints and their corresponding gapped counterparts were reported. The fatigue performances were assessed by comparing the SCF, HSS and actual fatigue life between a set of selected gapped and overlapped CHS-K joints with similar geometrical parameters. Both the SCF and the HSS comparisons yield consistent results and they indicated that partially overlapped CHS K-joints are better when working under the AX loading case. On the other hand, gapped CHS K-joints were found to be better when working under the IPB loading case. From the results obtained during fatigue life comparisons under different braces loading cases, despite the marginal effects of different sectional thickness of the joint members, it was found that the overlapped joints are still be favoured when dominating braces axial loadings are applied. Finally, it could be concluded that as during actual truss design most of the members will be assumed to be axially loading only, a partially overlapped CHS K-joints could be regarded as a favourite when comparing with its gapped counterpart in terms of fatigue performance.

Notations

The following symbols are used in this paper:

CHS	= Circular hollow section
AX	= Axial loading
IPB	= In-plane bending
SCF	= Stress concentration factor
HSS	= hot spot stress
D	= Diameter of Chord
d	= Diameter of braces
L	= Length of chord
g	= Gap distance between two braces for gapped joint
p	= Projection length of overlapped brace diameter on chord
q	= Length of overlap between two braces
O_v	= Overlapping ratio
T	= Thickness of chord
t	= Thickness of brace
α	= Chord length parameter
β	= Brace-to-chord diameter ratio
τ	= Brace thickness to chord thickness ratio
ζ	= Brace to chord width ratio
SCF_{Ov}	= Maximum SCF for the partially overlapped CHS K-joint
SCF_{Gap}	= Maximum SCF for the gapped CHS K-joint
$D_{Ov-Gap}(SCF)$	= Relative differences between the maximum SCF
HSS_{Ov}	= HSS for the partially overlapped CHS K-joint
HSS_{Gap}	= HSS for the gapped CHS K-joint
$D_{Ov-Gap}(HSS)$	= Relative differences between the HSS
F_{Ov}	= Numbers of cycles to failure for the partially overlapped CHS K-joint
F_{Gap}	= The numbers of cycles to failure for the gapped CHS K-joints
$D_{Ov-Gap}(FL)$	= Relative differences between the numbers of cycles to failure

References

- [1] EN 1993-1-9 (2005) Design of steel structures, Part 1.9: fatigue strength of steel structures. Brussels: CEN.
- [2] Zhao, X. L., Herion, S., Packer, J. A., Puthli, R., Sedlacek, G., Wardenier, J., Weynand, K., Wingerde, A. van and Yeomans, N., (2001), Design Guide 8, For CHS and RHS welded joints under fatigue loading. CIDECT, TÜV Verlag, Köln
- [3] Kurobane, Y. and Ochi, K., (1996) "AWS vs International Design Rules for circular tubular K-connections", Engineering Structures, 19(3), pp.259-66
- [4] Bouwkamp, J.G., (1964), "Concept of tubular-joint design, Proceedings ASCE", Journal of Structural Division, USA.
- [5] Tizani, W.M.K., Yusurf, K.O., Davies, G. and Smith, N.J., (1996), "A knowledge based system to support joint fabrication decision making at the design stage – case study for CHS trusses", Proceeding of the 7th International Symposium on Tubular Structures, Hungary, pp. 483-89.
- [6] Fessler, H., Little, W.J.G. and Shellard, I.J., (1979), "Elastic stress due to axial loading of tubular joints with overlap", BOSS'79, USA.
- [7] Gibstein, M.B., (1987), "Stress concentration in tubular k-joints with diameter ratio equal to one, steel in marine structures", Elsevier, Amsterdam, Netherlands, pp. 377-93
- [8] Efthymiou, M., and Durkin, S., (1985), "Stress concentrations in T/Y and Gap/Overlap K-joints, behavior of offshore structures", Elsevier, Amsterdam, Netherlands, pp. 429-40.
- [9] Dharmavasan, S. and Seneviratne, L.D., (1986), "Stress analysis of POCHS K-joints, Fatigue and Crack Growth in Offshore Structures", IMechE 1986-2, pp. 17-30.
- [10] Sopha T., Nguyen, T.B.N., Chiew, S.P., Lee, C.K. and Lie, S.T., (2008), "Stress analysis and fatigue test on partially overlapped CHS K-Joints", Advanced Steel Construction, Vol. 4, No. 2, pp. 134-46.
- [11] Moe, E.T., (1987), "Stress analysis and fatigue tests on overlapped k-joints", Steel in Marine Structures, Elsevier, Amsterdam, Netherlands, pp. 395-404.
- [12] Gho, W.M., Gao, F. (2004), "Parametric equations for stress concentration factors in completely overlapped tubular K(N)-joints", Journal of Constructional Steel Research, 60(12), pp. 1761-1782

- [13] Gho, W.M., Gao, F. and Yang, Y. (2006), "Strain and stress concentration of completely overlapped tubular CHS joints under basic loadings", *Journal of Constructional Steel Research*, 62(7), pp. 656-674
- [14] Gao, F. Shao, Y.B., Gho, W.M. (2007), "Stress and strain concentration factors of completely overlapped tubular joints under lap brace IPB load", *Journal of Constructional Steel Research*, 63(3), pp. 305-316
- [15] Pang, N.L, Zhao, X.L., Mashiri, F.R. and Dayawansa, P. (2009), "Full-size testing to determine stress concentration factors of dragline tubular joints", *Engineering Structures*, 31(1), pp.43-56
- [16] Mashiri, F.R., Zhao, X.L. and Grundy, P., (2004), "Stress concentration factors and fatigue behaviour of welded thin-walled CHS-SHS T-joints under in-plane bending, *Engineering Structures*, 26, pp.1861-75
- [17] Nguyen T.B.N., (2008), "Model and mesh generation of partially overlapped circular hollow section k-joints for fatigue studies", Ph.D. Thesis, Nanyang Technology University, Singapore.
- [18] Kuang, J.G., Potvin, A.B., Leick, R.D. and Kahlich, J.L., (1977), "Stress concentration in tubular joints", *Society of Petroleum Engineering, USA*, August, pp. 287-99
- [19] Wordsworth A.C, Smedley G.P., (1978), "Stress concentrations at unstiffened tubular joints," *European Offshore Steels Research Seminar, Proceedings, Paper 31*, Cambridge, U.K., November, 1978.
- [20] Wordsworth A.C., (1981), "Stress concentration factors at K and KT tubular joints", *Fatigue of Offshore Structural Steels, Conference Proceedings*, February, pp. 59-69.
- [21] Smedley, P. and Fisher, P., (1991), "Stress concentration factors for simple tubular joints", *Proceedings of the 1st International Offshore and Polar Engineering Conference*, Edinburgh, UK, ISOPE, pp. 475-83.
- [22] Karamanos, S. A., Romeijn, A. and Wardenier, J., (2000), "Stress concentrations in tubular gap K-joints: mechanics and fatigue design", *Engineering Structures*, 22, pp.4-14
- [23] Schumacher, A., (2003), *Fatigue behaviour of welded circular hollow section joints in bridges*, Phd thesis number 2727, École Polytechnique Fédérale De Lausanne, Switzerland

- [24] Schumacher, A. and Alain Nussbaumer, A., (2006), "Experimental study on the fatigue behaviour of welded tubular K-joints for bridges", Engineering Structures, 28, pp.745-755
- [25] Lie, S. T., Lee, C. K., Chiew, S. P., Shao Yongbo, (2005), "Mesh modelling of cracked uni-planar tubular K-joints", Journal of Constructional Steel Research. Vol. 61, No. 2, pp 235 - 264.
- [26] Chiew, S.P., Lee, C.K., Lie, S.T. and Nguyen, T.B.N., (2009), "Fatigue study of partially overlapped circular hollow section-joints, Part 2: Experimental study and validation of numerical models", Engineering Fracture Mechanics. Vol. 76. No. 15, pp. 2408-28
- [27] Lee, C.K., Chiew, S.P., Lie, S.T. and Nguyen, T.B.N., (2009), "Fatigue study of partially overlapped circular hollow section-joints, Part I: Geometrical models and mesh generation", Engineering Engineering Fracture Mechanics. Vol. 76. No. 16, pp. 2445-63
- [28] Lee, C.K., Chiew, S.P., Lie, S.T. and Nguyen, T.B.N., (2010), "Adaptive mesh generation procedures for thin-walled tubular structures". Finite Element in Analysis and Design. Vol. 46 No.1-2, pp. 114- 31
- [29] International Institute of Welding, IIW (2000), "Fatigue design procedure for welded hollow section joints: Recommendations of IIW subcommission XV-E ", Edited by X-L Zhao and J A Packer, Woodhead Publishing Limited, ISBN-13: 978 1 85573 522 4
- [30] Packer, J. A., Birkemoe, P. C. and Tucker, W. J., (1984), "Canadian implementation of CIDECT Monograph No 6", CIDECT report No 5AJ-84/9-E, IIW Doc. SC-XV-E-84-072

List of Figures

Figure 1. Basic notations used for the gapped and the partially overlapped CHS K-joints; (a) Gapped CHS K-joint; (b) Partially overlapped CHS K-joint

Figure 2. A 3D solid finite element mesh used for the analysis of partially overlapped CHS K-joint; (a) Typical mesh used; (b) Stress distribution from the FE model

Figure 3. Comparison of SCF under the AX1 load case

Figure 4. Comparison of SCF under the IPB1 load case

Figure 5. Comparison of SCF under the AX2 load case

Figure 6. Comparison of SCF under the IPB2 load case

Figure 7. Comparison of HSS under AX1 (200kN)

Figure 8. Comparison of HSS under IPB1 (45kNm)

Figure 9. Comparison of HSS under AX1 (200kN) + IPB1 (10kNm)

Figure 10. Comparison of HSS under AX1 (200kN) + IPB1 (25kNm)

Figure 11. Comparison of HSS under AX1 (200kN) + IPB1 (45kNm)

Figure 12. Comparison of fatigue life under AX1 (200kN)

Figure 13. Comparison of fatigue life under IPB(45kN)

Figure 14. Comparison of fatigue life under AX(200kN)+IPB(10kN)

Figure 15. Comparison of fatigue life under AX(200kN)+IPB(25kN)

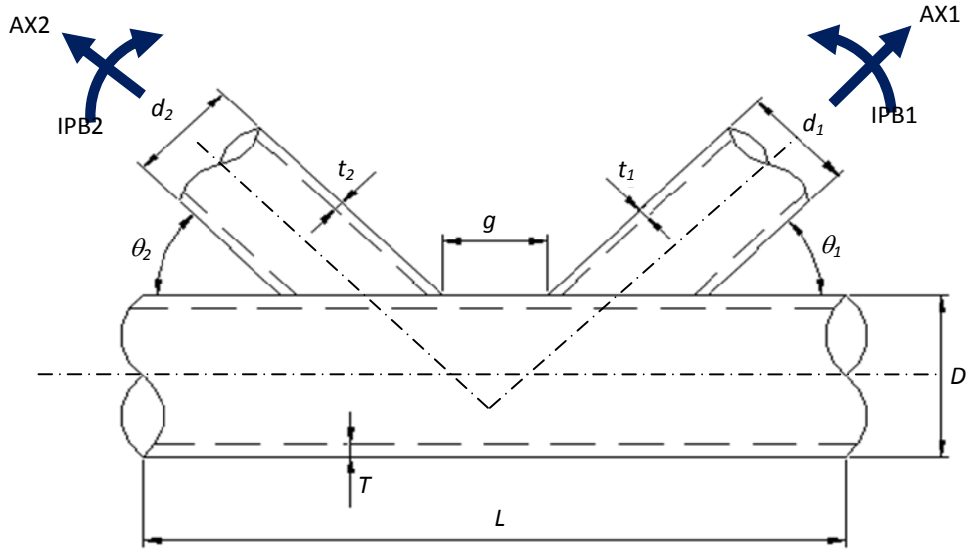
Figure 16. Comparison of fatigue life under AX(200kN)+IPB(45kN)

List of Tables

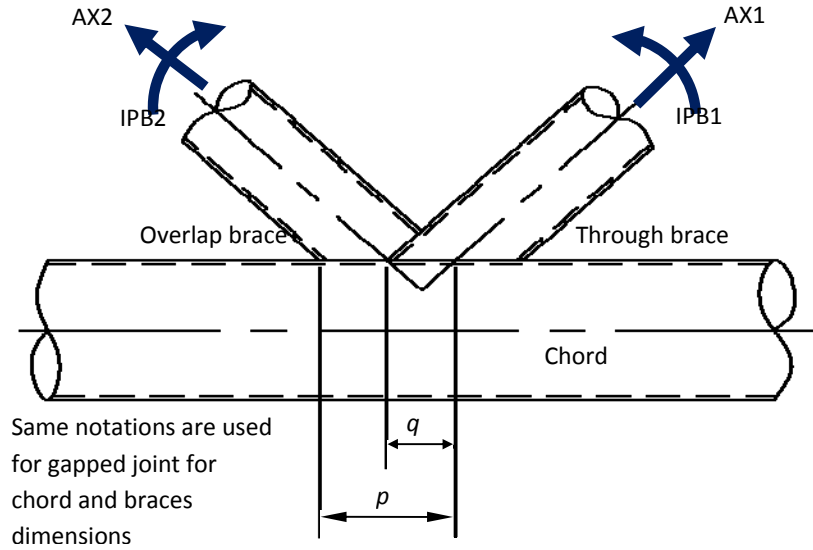
Table 1. Geometrical parameters of the 642 CHS K-joint configurations

Table 2a. DEn SCF equations for gapped CHS K-joints with identical braces

Table 2b Equations for the T, S, B and F factors used in Table 2a



(a) Gapped CHS K-joint

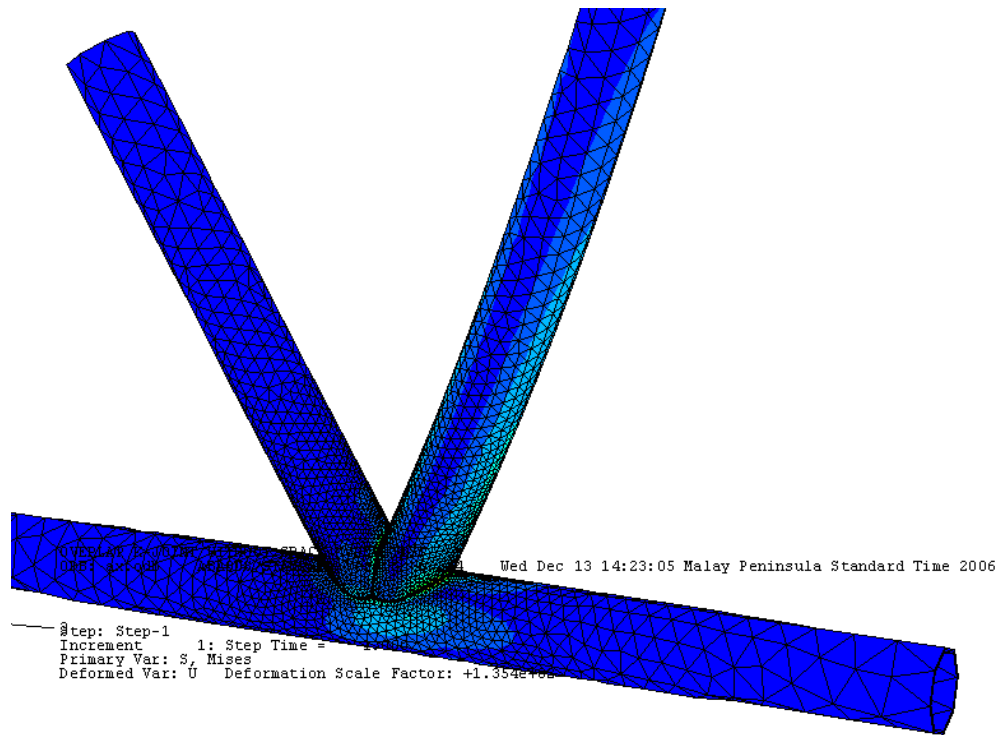


(b) Partially overlapped CHS K-joint and basic loading cases

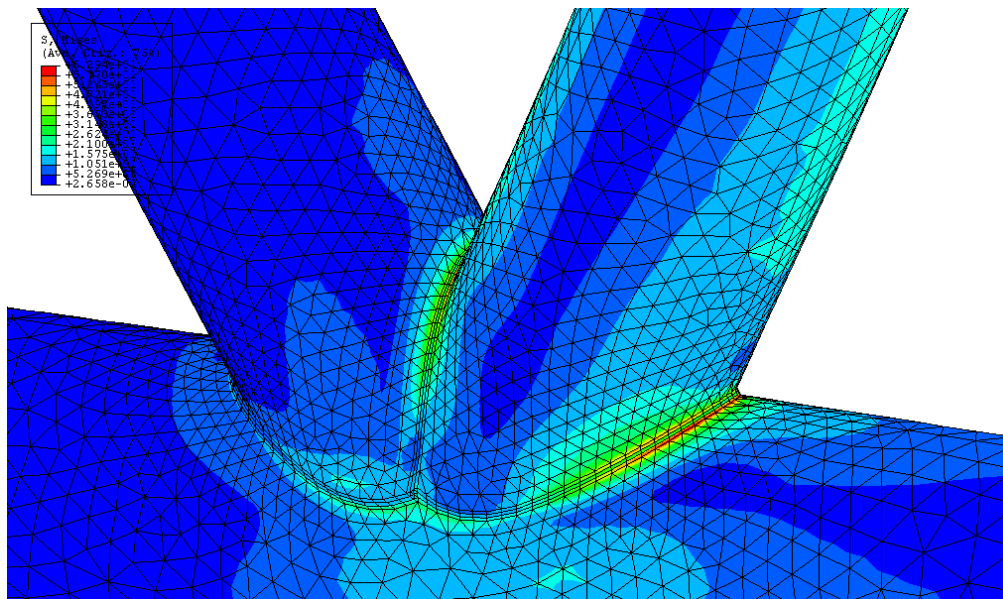
$$\alpha = \frac{2L}{D}, \gamma = \frac{D}{2t_0}, \beta_1 = \frac{d_1}{D}, \tau_1 = \frac{t_1}{T}, \beta_2 = \frac{d_2}{D}, \tau_2 = \frac{t_2}{T}$$

$$\zeta = \frac{g}{D} \text{ (for gap joint only), } O_v = \frac{p}{q} \text{ (for overlapped joint only)}$$

Figure 1. Basic notations for the gapped and the partially overlapped CHS K-joints



(a) Typical mesh used



(b) Stress distribution from the FE model

Figure 2. A typical 3D solid finite element mesh used for the analysis of partially overlapped CHS K-joint

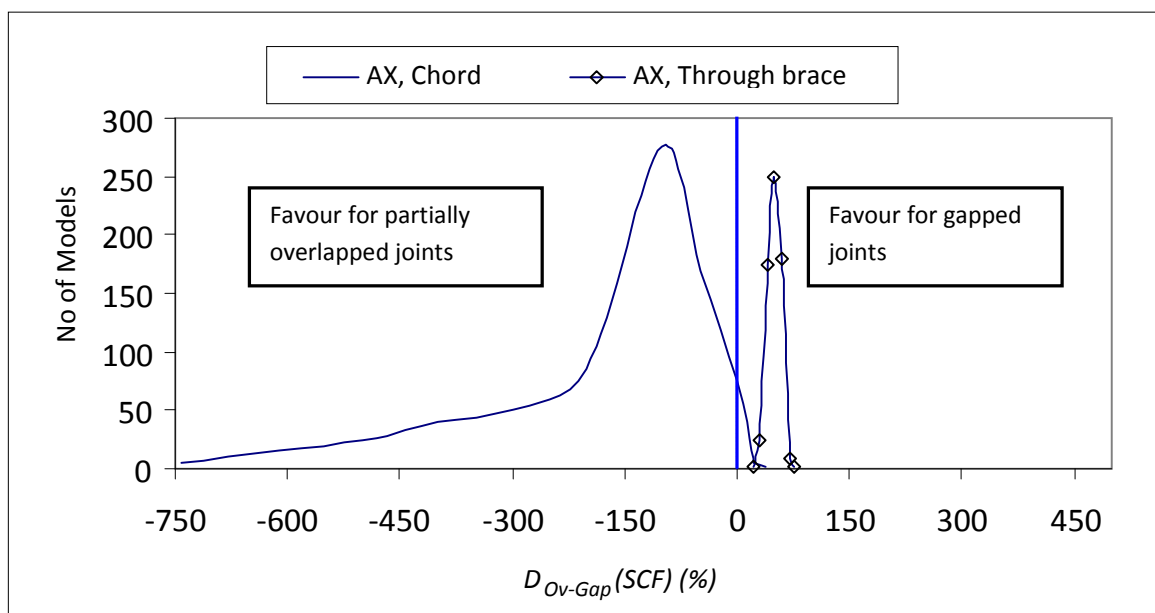


Figure 3. Comparison of SCF under the AX1 load case

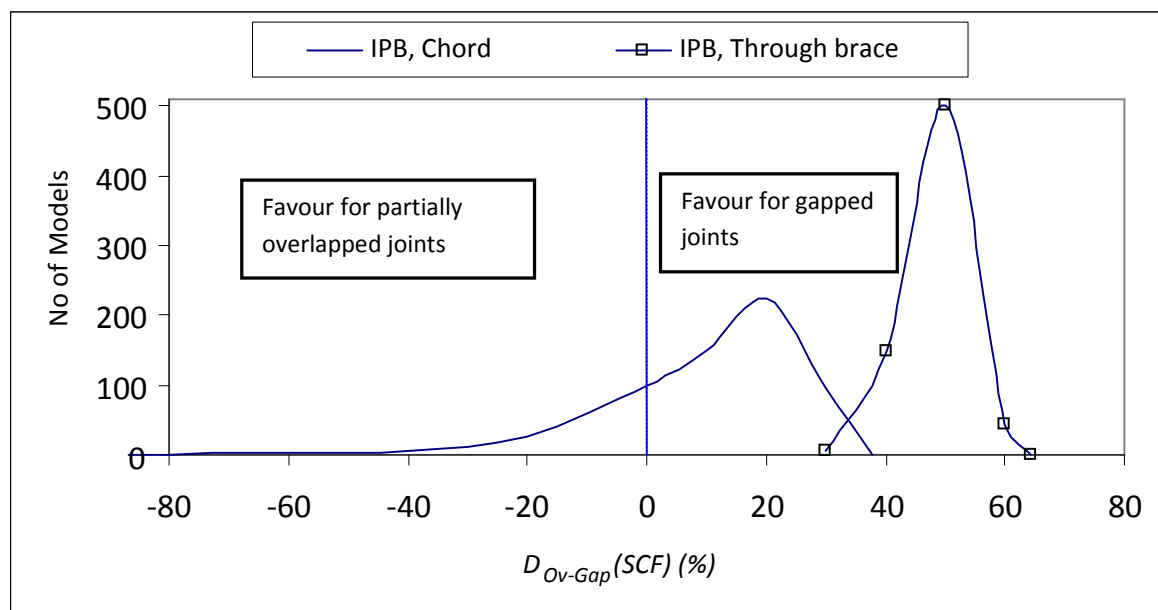


Figure 4. Comparison of SCF under the IPB1 load case

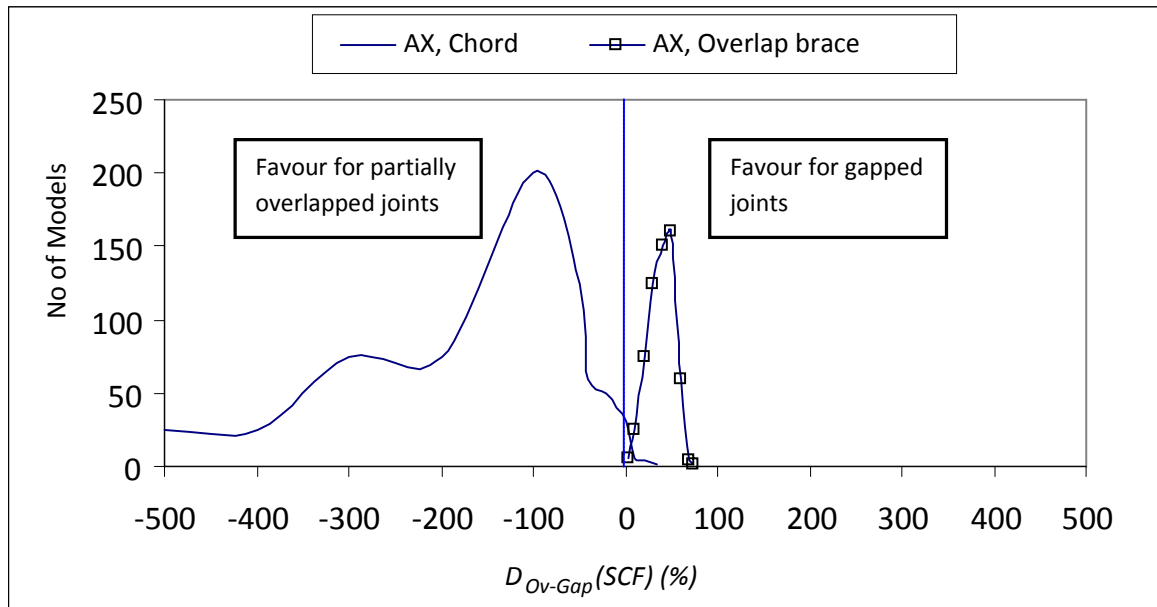


Figure 5. Comparison of SCF under the AX2 load case

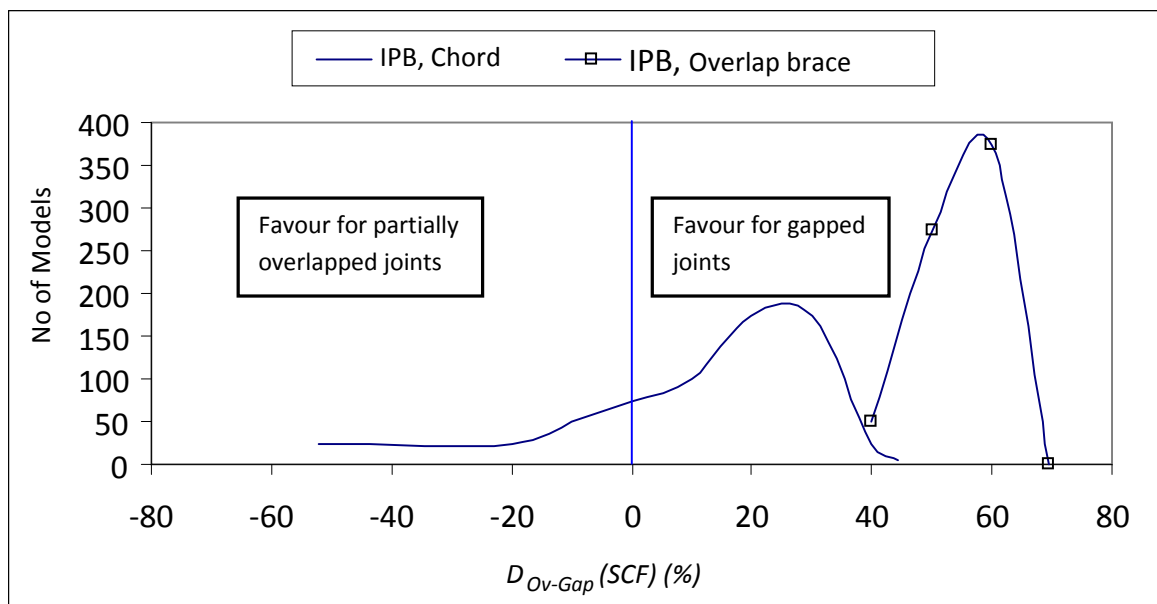


Figure 6. Comparison of SCF under the IPB2 load case

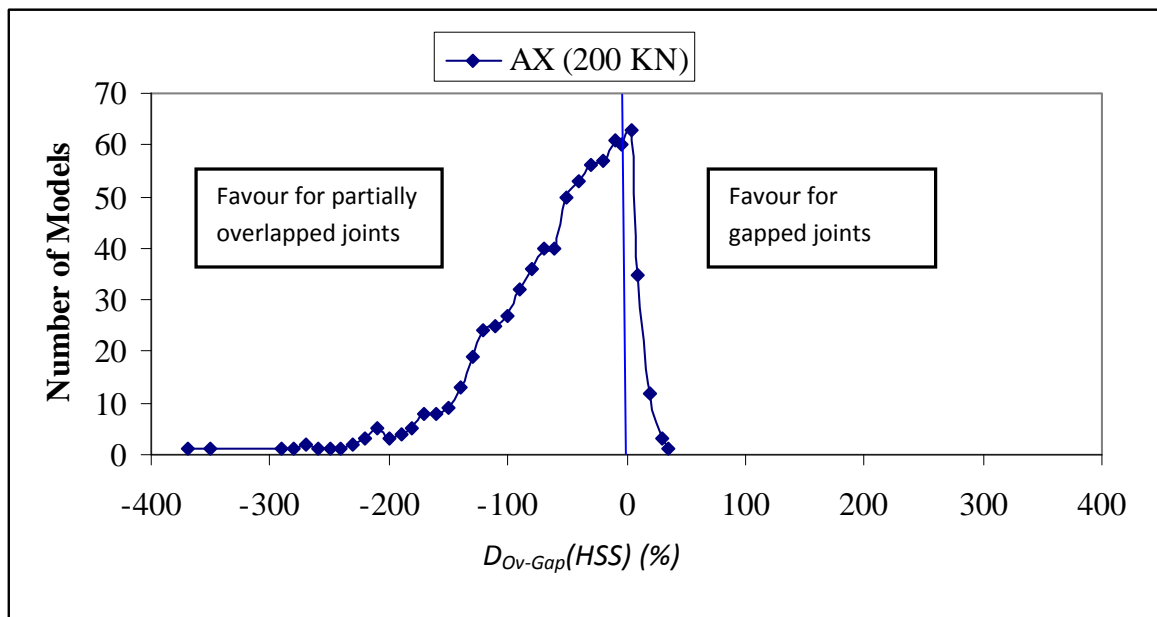


Figure 7. Comparison of HSS under AX1 (200kN)

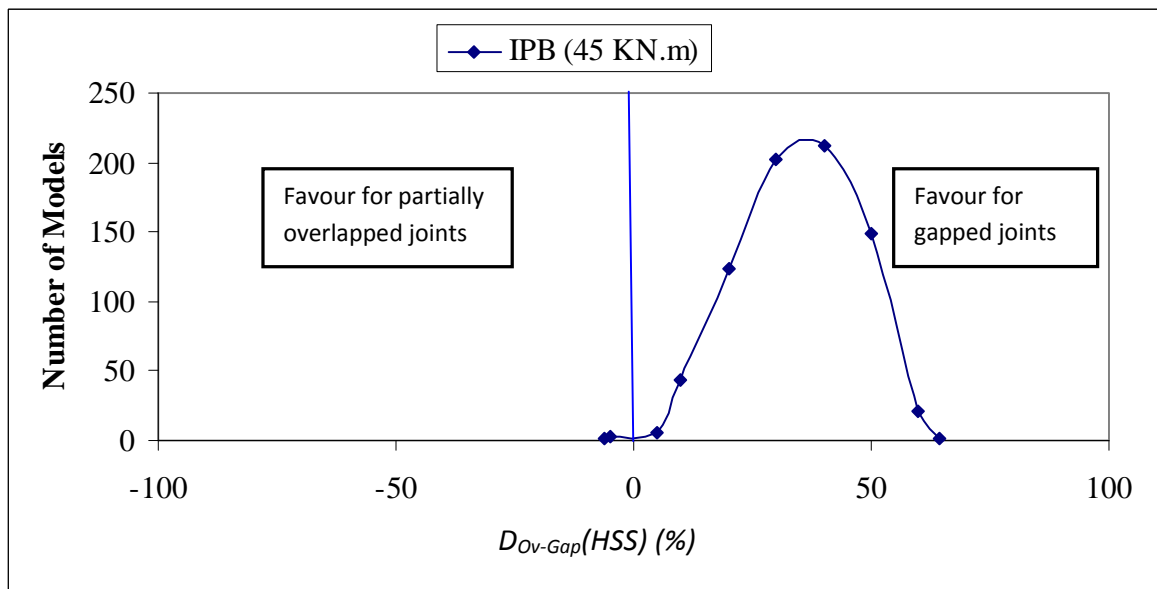


Figure 8. Comparison of HSS under IPB1 (45kNm)

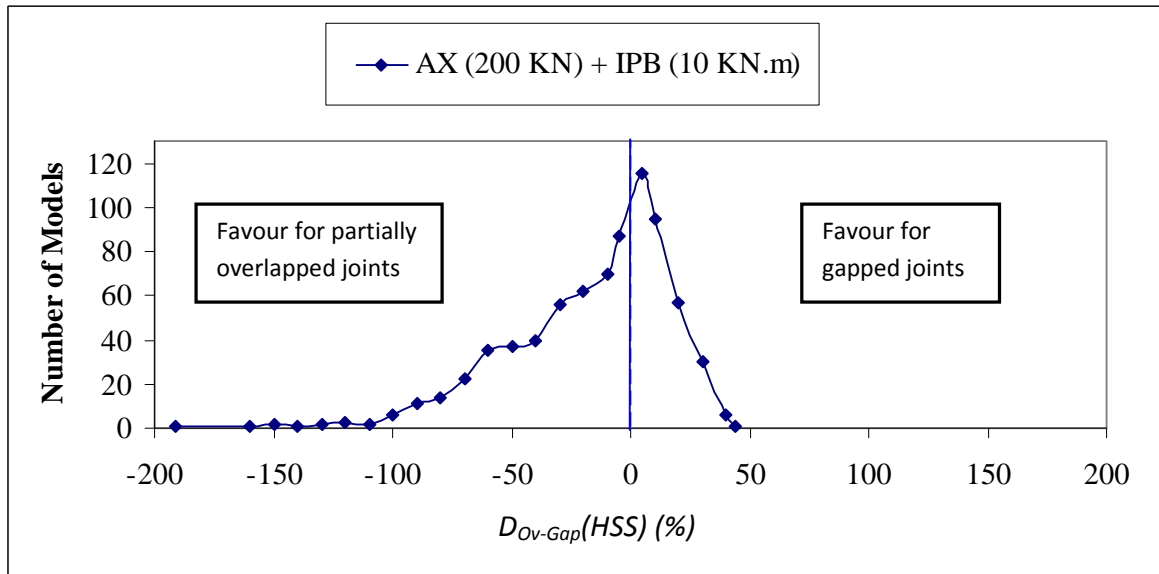


Figure 9. Comparison of HSS under AX1 (200kN) + IPB1 (10kNm)

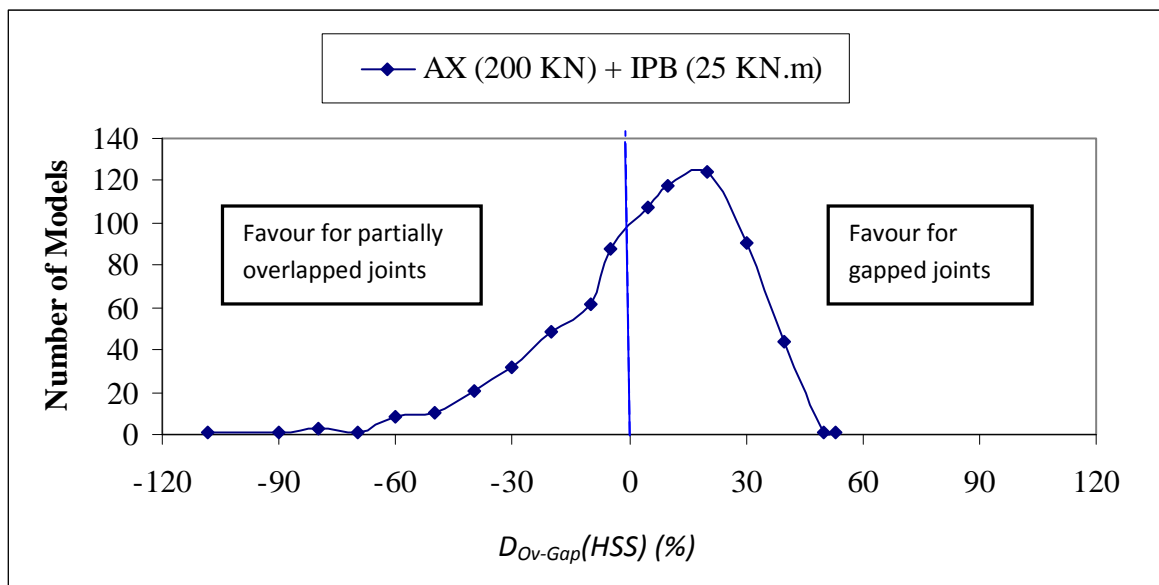


Figure 10. Comparison of HSS under AX1 (200kN) + IPB1 (25kNm)

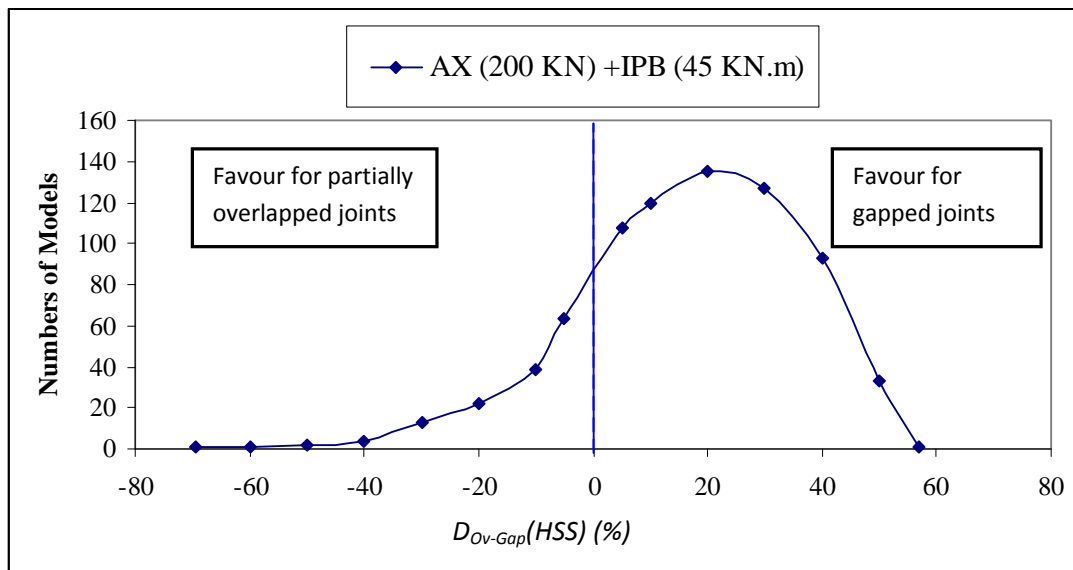


Figure 11. Comparison of HSS under AX1 (200kN) + IPB1 (45kNm)

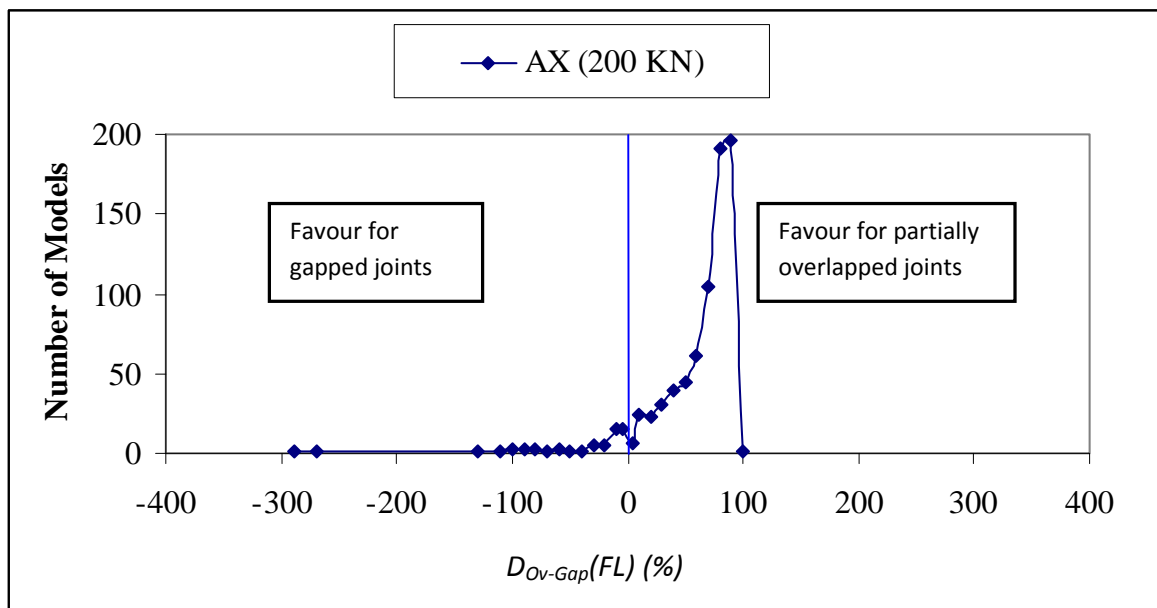


Figure 12. Comparison of fatigue life under AX1 (200kN)

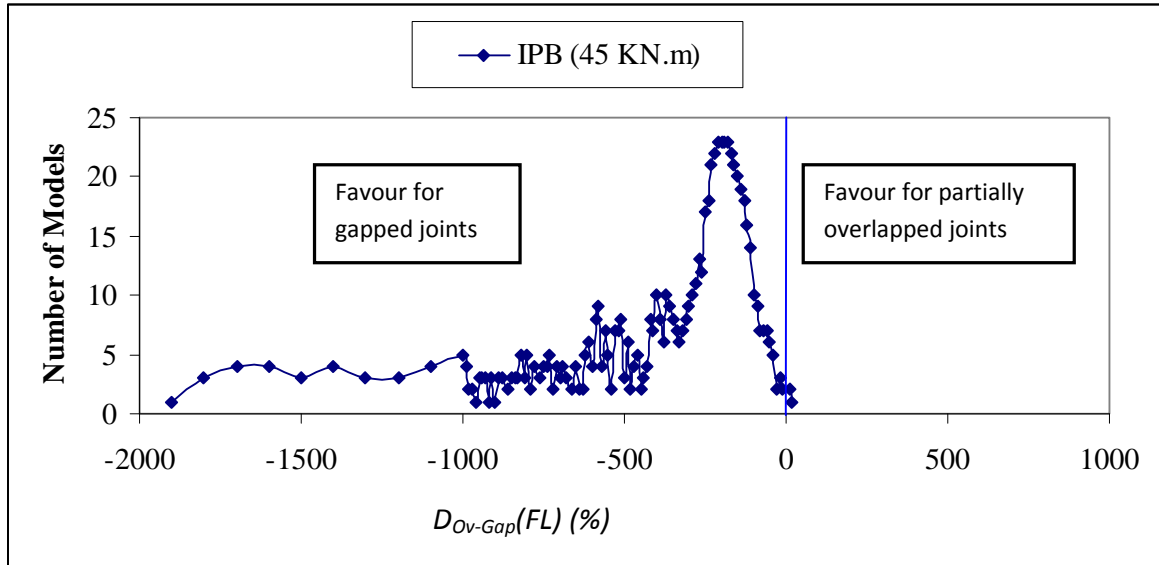


Figure 13. Comparison of fatigue life under IPB (45kNm)

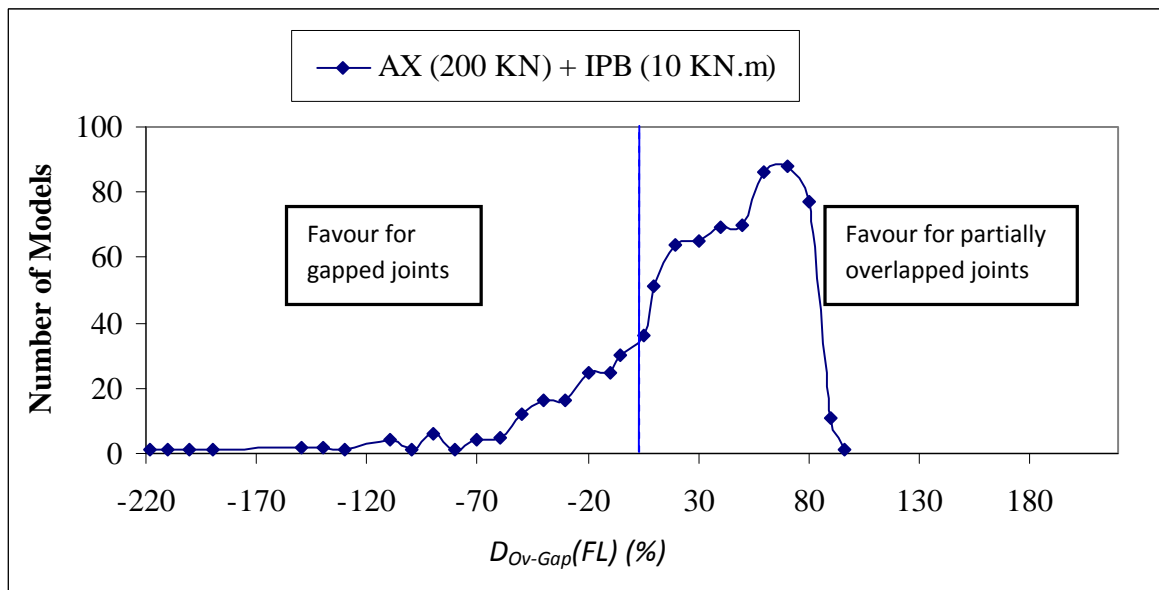


Figure 14. Comparison of fatigue life under AX (200kN)+IPB (10kNm)

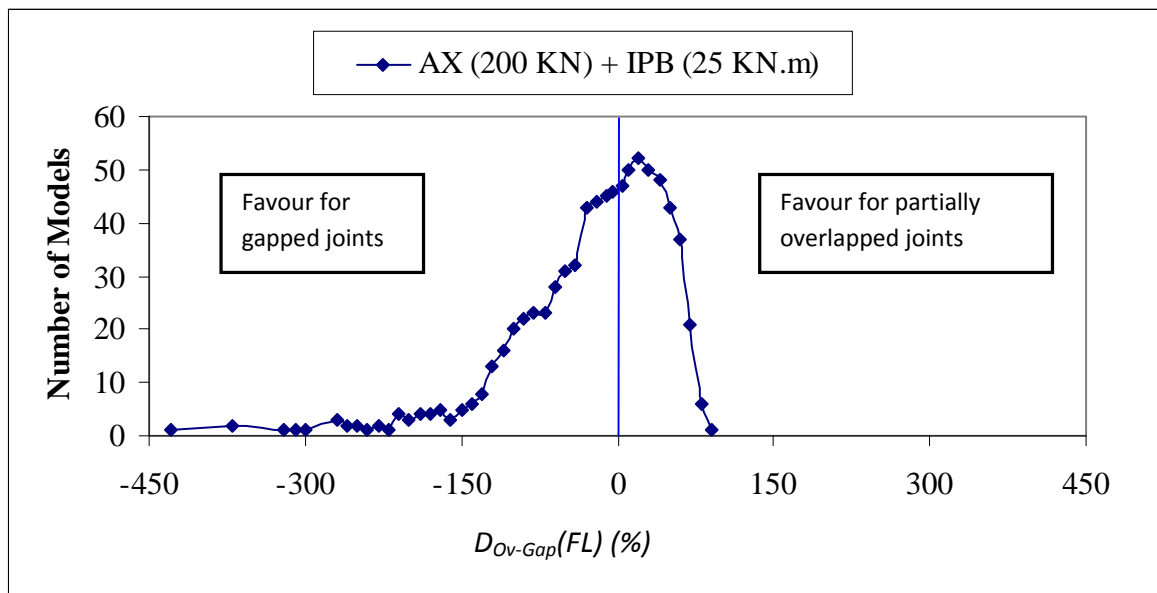


Figure 15. Comparison of fatigue life under AX (200kN)+IPB (25kNm)

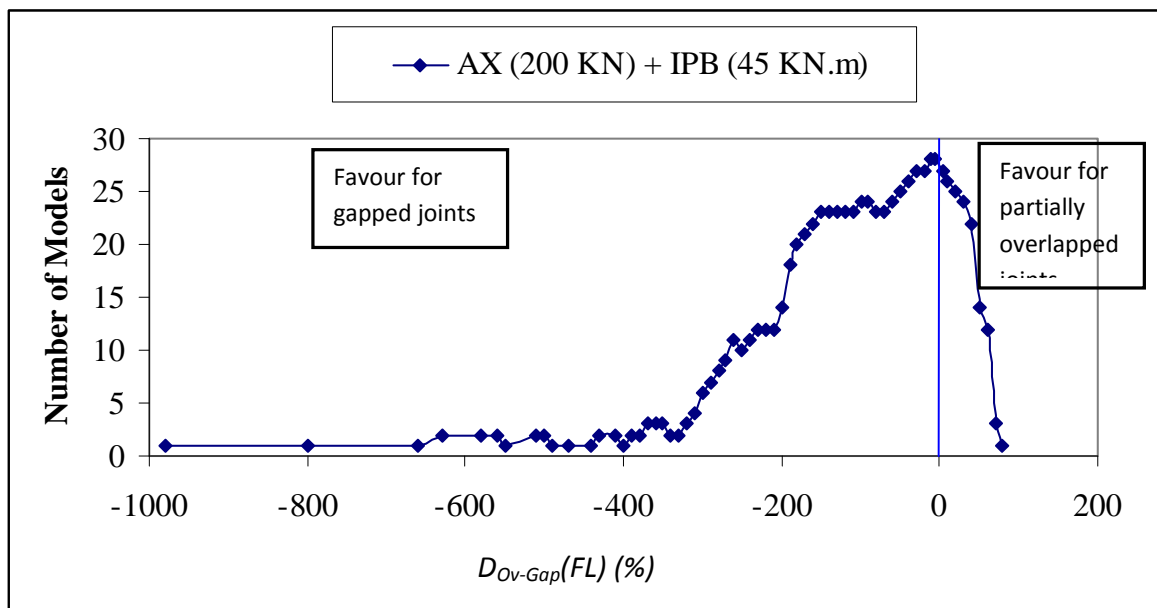


Figure 16. Comparison of fatigue life under AX (200kN)+IPB (45kNm)

Table 1 Geometrical parameters of the 642 CHS K-joint configurations (Groups 1 to 6)

Groups	β	O_v and θ	γ	T (mm)	τ (t/T)
Group 1 $D=355.6\text{mm}$ 87 Joints	0.91	0.45 and 60° ; 0.37 and 55° ; 0.29 and 50°	14.82	12	1
			14.22	12.5	0.8, 0.96, 1
			12.7	14	0.86, 0.89, 1.0
			12.52	14.2	0.85, 0.88, 0.99, 1.00
			11.11	16	0.63, 0.75, 0.78, 0.88, 0.89
			8.89	20	0.50, 0.60, 0.63, 0.70, 0.80, 1
			*7.11	25	0.48, 0.5, 0.56, 0.57, 0.64, 0.8, 1
Group 2 $D=273\text{mm}$ 50 Joints	0.9	0.36 and 55°	17.06	8	0.75, 0.79, 1
			13.65	10	0.8, 1
			11.38	12	0.5, 0.53, 0.67, 0.83, 1
			10.92	12.5	0.5, 0.64, 0.8, 0.96, 1
			9.75	14	0.57, 0.71, 0.86, 0.89, 1
			9.61	14.2	0.56, 0.85, 0.88, 0.99, 1
			8.53	16	0.38, 0.39, 0.50, 0.63, 0.75, 0.78, 0.88, 0.89, 1
			*6.83	20	0.3, 0.32, 0.4, 0.6, 0.63, 0.7, 0.71, 0.8, 1
Group 3 $D=177.8\text{mm}$ 21 joints	0.95	0.25 and 45°	*5.46	25	0.4, 0.48, 0.5, 0.56, 0.57, 0.64, 0.8
			14.82	6	1
			14.11	6.5	0.95, 1
			11.11	8	0.63, 0.75, 0.79, 1
			8.89	10	0.6, 0.63, 0.8, 1.00
			*7.41	12	0.5, 0.53, 1
Group 4 $D=193.7\text{mm}$ 87 joints	0.92	0.46 and 60° ; 0.38 and 55° ; 0.30 and 50°	*6.35	14	0.43, 0.45, 0.57, 0.71, 0.86, 0.89, 1
			16.14	6	1
			15.37	6.3	0.79
			12.11	8	0.75, 0.79, 1
			9.69	10	0.5, 0.6, 0.63, 0.8, 1
			8.07	12	0.53, 0.67, 0.83, 1
			*7.75	12.5	0.5, 0.64, 0.8, 0.96, 1
			*6.82	14.5	0.56, 0.70, 0.85, 0.88, 1
Group 5 $D=219.1\text{mm}$ 120 joints	0.88	0.43 and 60° ; 0.35 and 55° ; 0.27 and 50°	*6.05	16	0.5, 0.63, 0.75, 0.78, 0.89
			13.69	8	0.75, 0.79, 1
			10.96	10	0.5, 0.6, 0.63, 0.8, 1
			9.13	12	0.5, 0.53, 0.67, 0.83, 1
			8.76	12.5	0.5, 0.64, 0.8, 0.96, 1
			*7.71	14.2	0.42, 0.44, 0.56, 0.7, 0.85, 0.88, 1
			*6.85	16	0.38, 0.39, 0.5, 0.63, 0.75, 0.78, 0.89
Group 6 $D=193.7\text{mm}$ 87 joints	0.87	0.42 and 60° ; 0.34 and 55° ; 0.26 and 50°	*5.48	20	0.3, 0.32, 0.4, 0.5, 0.6, 0.63, 0.71, 0.8
			16.14	6	1.00
			15.37	8	0.79
			12.11	10	0.75, 0.79, 1
			9.69	12	0.5, 0.6, 0.63, 0.8, 1
			8.07	12.5	0.53, 0.67, 0.83, 1
			*7.75	14.2	0.5, 0.64, 0.8, 0.96, 1
			*6.82	16	0.56, 0.70, 0.85, 0.88, 1
			*6.05	20	0.5, 0.63, 0.75, 0.78, 0.89

Table 1 Geometrical parameters of 642 CHS K-joint configurations (Continued, Groups 7 to 14)

Groups	β	O_v and θ	γ	T (mm)	τ (t/T)
Group 7 $D=219.1\text{mm}$ 26 joints	0.84	0.35 and 60°	16.2	8	1
			13.5	10	0.83, 1
			12.96	12	0.80, 0.96, 1
			11.57	12.5	0.86, 0.89, 1
			11.40	14	0.85, 0.88, 0.99, 1
			10.12	14.2	0.5, 0.63, 0.75, 0.78, 0.88, 0.89
			8.10	16	0.4, 0.5, 0.6
			*6.48	20	0.32, 0.4, 0.48, 0.5
Group 8 $D=168.3\text{mm}$ 34 joints	0.83	0.40 and 60° ; 0.31 and 55°	14.30	6	1
			13.36	6.3	0.95, 1
			10.52	8	0.75, 0.79, 1
			8.42	10	0.6, 0.63, 0.8
			*7.01	12	0.53, 0.67, 0.83, 1
			*6.01	14	0.71, 0.86, 0.89, 1
Group 9 $D=139.7\text{mm}$ 26 joints	0.82	0.39 and 60° ; 0.30 and 55°	11.09	6.3	0.95, 1
			8.73	8	0.75, 0.79, 1
			*6.99	10	0.60, 0.63, 0.8, 1
			*5.82	12	0.53, 0.67, 0.83, 1
Group 10 $D=177.8\text{mm}$ 29 joints	0.77	0.25 and 55°	14.82	12	1
			14.22	12.5	0.8, 0.96, 1
			12.7	14	0.86, 0.89, 1
			12.52	14.2	0.85, 0.88, 0.99, 1
			11.11	16	0.63, 0.75, 0.78, 0.88, 0.89
			8.89	20	0.50, 0.60, 0.63, 0.70, 0.80, 1
			*7.11	25	0.48, 0.5, 0.56, 0.57, 0.64, 0.8, 1
Group 11 $D=168.3\text{mm}$ 13 joints	0.73	0.31 and 60°	11.09	6.3	0.95, 1
			8.73	8	0.75, 0.79, 1
			*6.99	10	0.60, 0.63, 0.8, 1
			*5.82	12	0.53, 0.67, 0.83, 1
Group 12 $D=193.7\text{mm}$ 24 joints	0.75	0.34 and 60°	16.2	10	0.8, 1
			13.5	12	0.83, 1
			12.96	12.5	0.8, 1
			11.57	14	0.86, 0.89
			11.40	14.2	0.85, 0.88
			10.12	16	0.5, 0.63, 0.75, 0.78
			8.10	20	0.4, 0.5, 0.6, 0.63, 1
			*6.48	25	0.32, 0.4, 0.5, 0.64, 0.8
Group 13 $D=193.7\text{mm}$ 22 joints	0.72	0.31 and 60°	16.14	6	1
			15.37	6.3	1
			12.11	8	0.75, 0.79, 1
			9.69	10	0.6, 0.63, 0.8, 1
			8.07	12	0.5, 0.53, 0.67, 0.83
			*7.75	12.5	0.48, 0.5, 0.64
			*6.82	14.2	0.42, 0.44, 0.56, 0.7
			*6.05	16	0.5, 0.63
Group 14 $D=168.3\text{mm}$ 16 joints	0.68	0.26 and 60°	13.36	6.3	0.95, 1
			10.52	8	0.75, 0.79, 1
			8.42	10	0.6, 0.63, 0.8
			*7.01	12	0.53, 0.67, 0.83, 1
			*6.01	14	0.71, 0.86, 0.89, 1

*Cases where the results for the gapped joint were obtained by finite element modellings.

Table 2a. DEn SCF equations for gapped CHS K-joints with identical braces

Load type	SCF equations
AX loading on one brace only (AX1 or AX2)	$SCF_{CS} = 1.18 \times T1 \times S1 \times (F1 \text{ or } F2)$ $SCF_{CC} = 1.13 \times T2 \times S2 + B0 \times B1$ $SCF_{BS} = 1.20 \times T3 \times S1 \times (F1 \text{ or } F2)$ $SCF_{BC} = 1.23 \times T4 \times S2$
IPB loading on one brace only (IPB1 and IPB2)	$SCF_C = 1.15 \times T5$ $SCF_B = 1.17 \times T6$

Legend for Table 2a

 SCF_{CS} =SCF at the chord saddle SCF_{CC} =SCF at the chord crown SCF_{BS} =SCF at the brace saddle SCF_{BC} =SCF at the brace crown SCF_C =Maximum SCF on the chord side SCF_B =Maximum SCF on the brace sideTable 2b Equations for the T , S , B and F factors used in Table 2a

T Factors	$T1 = \tau \gamma^{1.2} (2.2\beta - 2\beta^2) \sin^2 \theta$; $T2 = \tau \gamma^{0.2} (3.5\beta - 2.4\beta^2) \sin^{0.3} \theta$ $T3 = 1 + \tau^{0.2} \gamma^{1.3} (0.76\beta - 0.7\beta^2) \sin^{2.2} \theta$; $T4 = 2.6\beta^{0.8} \gamma^{(1-0.68\beta)} \sin^{(1-\beta^2)} \theta$ $T5 = 1.22\tau^{0.8} \beta \gamma^{(1-0.68\beta)} \sin^{(1-\beta^3)} \theta$; $T6 = 1 + \tau^{0.2} \gamma \beta (0.26 - 0.21\beta) \sin^{1.5} \theta$
S Factors	$S1 = \left[1 - 0.4 \exp \left(-30x^2 \left(\frac{\sin \theta}{\gamma} \right) \right) \right]$; $S2 = \left[1 + 0.4 \exp \left(-2x^2 \left(\frac{1}{\gamma^{0.5} \sin^2 \theta} \right) \right) \right]$
B Factors	For single axial load: $B0 = \frac{C\tau(\beta - \tau/(2\gamma))(\alpha/2 - \beta/\sin \theta)\sin \theta}{(1 - 3/(2\gamma))}$ For balanced axial load: $B0 = 0$ $B1 = 1.05 + \frac{30\tau^{1.5} (1.2 - \beta) \cos^4 \theta + 0.15}{\gamma}$; $C = \begin{cases} 0.5 & \text{for fully fixed chord ends} \\ 1.0 & \text{for pinned chord ends} \\ 0.7 & \text{for other cases} \end{cases}$
F Factors	For $\alpha \geq 12$: $F1=F2=1.0$ For $\alpha < 12$: $F1 = 1 - (0.83\beta - 0.56\beta^2 - 0.02)\gamma^{0.23} \exp(-0.21\gamma^{(-1.16)}\alpha^{2.5})$ $F2 = 1 - (1.43\beta - 0.97\beta^2 - 0.03)\gamma^{0.04} \exp(-0.71\gamma^{(-1.38)}\alpha^{2.5})$

Validity range for equation shown in Tables 2a and 2b:

 $0.13 \leq \beta \leq 1.00$; $10.0 \leq \gamma \leq 35$; $0.25 \leq \tau \leq 1.00$; $30^\circ \leq \theta \leq 90^\circ$; $4.0 \leq \alpha$; $0.00 \leq \zeta \leq 1.00$